Organic & Biomolecular Chemistry

Accepted Manuscript

ROYAL SOCIETY OF CHEMISTRY

www.rsc.org/obc

Journal Name

ARTICLE

Catalytic chemodosimeteric approach for detection of nanomolar cyanide ions in water, blood serum and live cell imaging

Received 00th January 20xx,
Accepted 00th January 20xx

DOI: 10.1039/x0xx00000x

www.rsc.org/

Rahul Kumar[a], Sana Sandhu[a], Geeta Hundal[a], Prabhpreet Singh[a]*, Vanita Vanita[b], Amandeep Walia[b], and Subodh Kumar[a]*

Naphthimidazolium based monocationic chemodosimeters **CD-1** and **CD-2** undergo cyanide mediated catalytic transformation in the presence of cyanide ions (0.01% to 1% of **CD-1/ CD-2** concentration) with turnover number from 70 to 360. These chemodosimeters can detect as low as 0.5 nM and 1 nM cyanide ions under nearly physiological conditions (HEPES buffer – DMSO (5%), pH 7.4). The structures of **CD-1** and its cyanide induced hydrolyzed product **4** have been confirmed by single crystal X-ray crystallography. **CD-1** can also be used for the determination of 2 nM cyanide in the presence of blood serum. **CD-1** and **CD-2** also find applications in live cell imaging of 10 nM cyanide ions in rat brain C6 glioma cells. To the best of our knowledge, this is first report where high sensitivity towards cyanide ions has been achieved through catalytic hydrolysis of the fluorescent chemodosimeter.

Introduction

Since Czarnik et al's first report on a chemodosimeter[1] for Cu^{2+}, an extensive applications of chemodosimeters in literature[2,3] have appeared for the estimation of both metal ions and anions. In most of these cases, a chemodosimeter reacts with equimolar or larger quantities of an analyte to give the product with a change in fluorescence signal. However, in case, an analyte acts as a catalyst to transform the chemodosimeter to permit an analyte's turnover, a large increase in the fluorescence intensity even with sub-equimolar quantities of the analyte is observed and it results in amplification of the fluorescence signal. In spite of its distinct advantage, only a few reports on estimation of metal ions[4,5] viz. Pd(0), Pt(0), Cu^{2+}, Hg^{2+} and Au(III) using a catalytic chemodosimeteric approach have appeared in literature. Amongst anions, no report on catalytic version of chemodosimeters for anions or especially cyanide is reported.

Cyanide is considered to be most toxic of all anions and its toxic effects in blood can be observed at ~ 19 µM and can be lethal to humans at concentrations as low as 115 µM or 0.5–3.5 mg/Kg body weight[6]. Cyanide binds with Fe^{3+} of heme unit, and affects the oxygen supply[7]. It also causes cellular death by inactivating the active site of cytochrome c and blocking the electron transport chain resulting in inhibition of cellular respiration[8]. Cyanide has been also used as a chemical warfare reagent, and even as terror material[9]. Despite such a detrimental effect on human health, cyanide as a reagent has been used widely in paper, textiles and plastics manufacturing processes[10].

The seeds of several fruits including apricots, apples and peaches contain substantial amounts of biochemicals that release cyanide when metabolized. Accumulation of cyanide in humans could also happen through consumption of such foods and plants[11]. Its acute toxicity accounts for a very low tolerance limit and according to the regulatory bodies (U.S. EPA) the maximum acceptable level of cyanide in drinking water and environmental primary standard is 0.2 and 0.5 ppm, respectively[12]. Therefore, the effluents from these processes always need to be tested[13] for >1 µM (>26 ppb) concentrations of cyanide.

Though cyanide under biological conditions undergoes metabolism to thiocyanate and 2-aminothiazoline-4-carboxylic acid which have found some applications as biomarkers[14], but the most appropriate target for diagnosis of cyanide exposure remains the direct analysis of cyanide. Therefore, easy and affordable detection methods for cyanide are in great demand for various situations.

Dasgupta et al[15] have developed an integrated cyanide capture "apparatus", consisting of sample and cyanide capture chambers, for rapid separation of cyanide from blood samples and its quantification by measuring a change in the absorbance of cobinamide. Logue et al[16] have used similar device involving conversion of naphthalene dialdehyde, taurine, and cyanide, to fluorescent β-isoindole for emission based determination of cyanide from the blood samples but such approaches have limitation for live cell imaging of cyanide.

[a] Department of Chemistry, UGC Centre for Advanced Studies, Guru Nanak Dev University, Amritsar 143 005, India.
[b] Department of Human Genetics, Guru Nanak Dev University, Amritsar 143 005, India.
email address: subodh_gndu@yahoo.com; prabhpreet.chem@gndu.ac.in
Corresponding author. Mobile: +91 9872361528.
Electronic Supplementary Information (ESI) available: [details of any supplementary information available should be included here]. See DOI: 10.1039/x0xx00000x

Though for more than 175 years[17] cyanide is known to act as catalyst in benzoin condensation reaction, all the reported cyanide chemodosimeters[18,19] depend on the addition of cyanide to electron-deficient carbon-carbon double bond, carbon-heteroatom double bond. In other approaches, Sessler et al.[20] have used benzil rearrangement and benzil cyanide reactions on 1,2-dicarbonyl derivatives to develop a dosimeter-type detection of CN^- ions. Elsner reaction[21] between cyanide and gold atoms has been used to develop fluorescent chemodosimeters for CN- ions.

Recently, we have reported[22] that 1-(4-nitrophenyl)-benzimidazolium derivatives (scheme 1) undergo nucleophilic addition of cyanide at C-2 of benzimidazolium cation to form an adduct which subsequently undergoes hydrolysis under aqueous conditions to give the respective formamide derivatives and free cyanide is released. However in spite of release of CN- ion during hydrolysis, the chain or catalytic reaction of cyanide on another benzimidazolium molecule is not observed. Significantly, respective imidazolium derivatives do not undergo addition of cyanide ion (scheme 1). We envisaged that if the rate of these processes is increased, the released cyanide ions may react repeatedly to hydrolyze the respective naphthimidazolium derivatives and as a result a catalytic chemodosimeter, the first of its kind for the anions, will be produced.

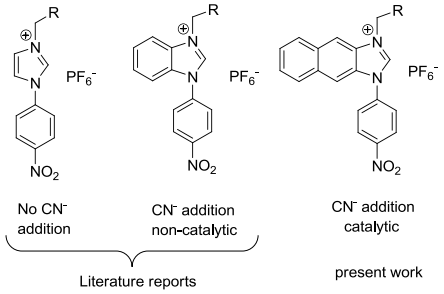

Scheme 1. Structural comparison of chemodosimeters.

We now hereby report that naphthimidazolium based monocationic chemodosimeters **CD-1** and **CD-2** undergo cyanide mediated catalytic transformation in the presence of 0.01% to 1% cyanide ions with turnover number from 70 to 360. These chemodosimeters can detect as low as 0.5 nM and 1 nM cyanide ions under nearly physiological conditions (HEPES buffer -5% DMSO, pH 7.4). Chemodosimeter **CD-1** can also be used for the determination of 2 nM cyanide in the presence of blood serum. These also find applications in live cell imaging of 10 nM cyanide ions in rat brain C6 glioma cells. To the best of our knowledge, this manuscript accomplishes first report where high sensitivity towards cyanide ions has been achieved through catalytic hydrolysis of the fluorescent chemodosimeter. The structures of the probes and the hydrolysed products have been unequivocally proved by single crystal X-ray crystallography in the solid state and using ^{1}H NMR, HRMS and photophysical studies in the solution phase.

Results and discussion

The chemodosimeters **CD-1** and **CD-2** were synthesized as given in scheme 2. The 1:1 stoichiometric solution of compounds **1** and **2** in acetonitrile on refluxing for 24 h gave solid product which was subjected to anion exchange with PF_6^- to get chemodosimeter **CD-1**, yellow solid; 90% yield. In its ^{1}H NMR spectrum, the presence of NCH_2 signal at δ 6.74 and naphthimidazolium C2-H singlet at δ 8.97 along with other aromatic signals due to naphthimidazolium and nitrophenyl groups confirms the formation of **CD-1**. Similarly, the reaction of **1** with 1-bromomethylpyrene (**3**) in acetonitrile at reflux temperature with subsequent exchange of anion with PF_6^- gave chemodosimeter **CD-2,** in 90% yield. For spectral data see SI (figure SI 1-10).

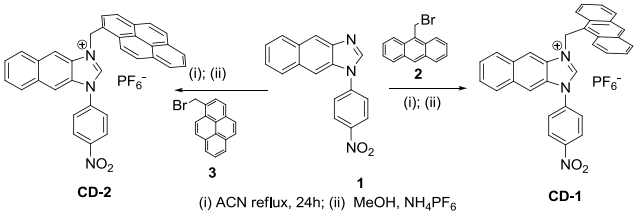

Scheme 2. Synthesis of chemodosimeters **CD-1** and **CD-2**.

To study the behaviour of **CD-1** towards various anions, the solutions of **CD-1** (5 μM, HEPES buffer – 5% DMSO, pH 7.4) and its mixtures with various anions (100 μM each) were prepared and their absorption and emission spectra were recorded. The UV-Vis spectrum of solution of **CD-1** shows characteristic absorption bands at 353 (ϵ 15200), 377 (ϵ 17400) and 393 (ϵ 16600) nm due to anthracene moiety. Amongst various anions, only on addition of NaCN (10 μM), the significant increase in absorbance at 353, 377, 393 nm was observed along with increase in absorbance between 400-450 nm (figure SI 11a). The latter could be attributed to increased ICT from nitrogen to *p*-nitrophenyl ring.

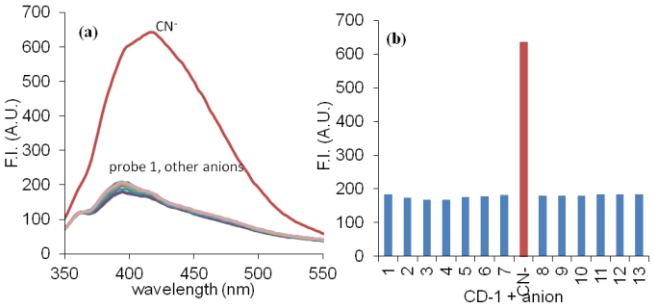

Figure 1. (a) Effect of various anions (100 μM) on the emission spectrum (λ_{ex} 320 nm) of chemodosimeter **CD-1** (5 μM, HEPES buffer -5% DMSO, pH 7.4), (b) change in fluorescence intensity on addition of various anions 1 = **CD-1**, 2 = **CD-1** + F^-, 3 = **CD-1** + Cl^-, 4 = **CD-1** + Br^-, 5 = **CD-1** + I^-, 6 = **CD-1** + ClO_4^-, 7 = **CD-1** + NO_3^-, 8 = **CD-1** + $H_2PO_4^-$, 9 = **CD-1** + HSO_4^-, 10 = **CD-1** + SO_4^{2-}, 11 = **CD-1** + OH^-, 12 = **CD-1** + SCN^-, 13 = **CD-1** + AcO^-.

On excitation at 320 nm, the solution of **CD-1** showed a broad emission band between 350 - 550 nm, which exhibited nearly 200% increase in the emission intensity only on addition of NaCN (10 μM) (figure 1), whereas the addition of other anions viz. F^-, Cl^-, Br^-, I^-, NO_3^-, OH^-, AcO^-, $H_2PO_4^-$, SCN^-, HSO_4^-, SO_4^{2-} and ClO_4^- even in excess (100 μM) caused insignificant change in the fluorescence intensity of **CD-1** (figure 1).

Further, to explore the applicability of **CD-1** towards estimation of CN^- ions, the fluorescence titration of **CD-1** with NaCN was carried out in the cuvette of spectrophotometer (figure 2). The fluorescence spectra were recorded after 2 min of addition of each aliquot of cyanide solution. It was observed that the gradual addition of 0-5 nM of NaCN to the solution of **CD-1** (5 μM, HEPES buffer - 5% DMSO) resulted in ~50% increase in the fluorescence intensity (FI) and corresponding to ~36% of the total increase in FI observed on addition of 5 μM of NaCN (figure 2c). Further, addition of up to 50 nM of NaCN, ~ 140% increase in FI was observed which accounted for ~70% of the total increase in FI observed on addition of 5 μM of NaCN (figure 2d) and residual ~ 30% enhancement in FI was observed on addition of 5 μM (1 equiv.) of NaCN and then a plateau was achieved (figure 2b). This was associated with ~ 13 times increase in fluorescence quantum yield[23] from 0.003 to 0.04 and the resulting solution appeared fluorescent blue in color to the naked eye under the illumination of 365 nm light (inset, figure 2b). The minimum detection limit[24] for the estimation of cyanide ions using **CD-1** was found to be 0.5 nM.

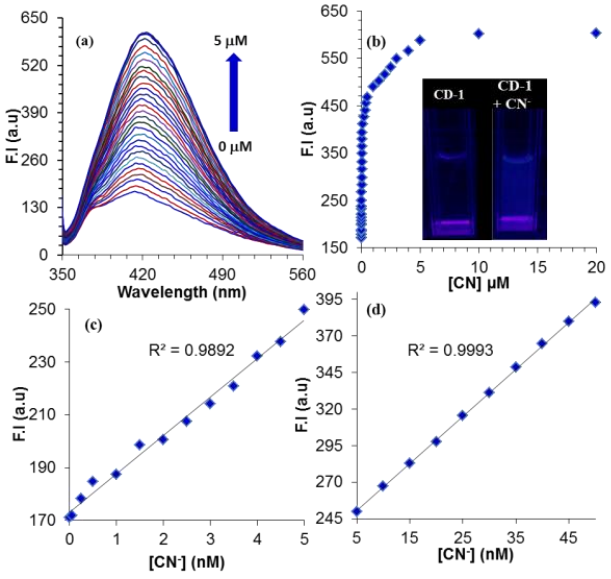

Figure 2. (a) Effect of gradual addition of NaCN on the emission spectrum (λ_{ex} 320 nm) of **CD-1** (5 μM, HEPES buffer - 5% DMSO, pH 7.4); (b) gradual change in fluorescence intensity of **CD-1** on addition of 0-5 μM NaCN, Inset shows the color of the solution of **CD-1** before and after addition of CN^- (5 μM) under illumination at 365 nm UV light; (c and d) show linear increase in FI with gradual increase in NaCN concentration between 0-5 nM and 5-50 nM, respectively.

These results clearly indicate that for the initial addition of 0-50 nM cyanide ions to the solution of **CD-1** (5 μM), the change in fluorescence intensity is nearly 70% of the maximum change in fluorescence intensity achieved on addition of 5000 nM (5 μM) cyanide ions (1 equiv.) and cyanide ions act as turn over catalyst for **CD-1** between 0-50 nM [CN^-]. The plot of fluorescence intensity vs [CN^-] shows linear relationship between 0-5 nM [CN^-] with R^2 = 0.9892 (figure. 2c) and 36% molecules of **CD-1** out of 5 μM are converted to open molecule **4** (scheme 3). This clearly points to turnover number (TON) ~ 360 for cyanide ions to cause hydrolysis of **CD-1**. Between additions of 5 nM to 50 nM cyanide ions, the ratio FI / [cyanide] was lowered and turnover number (TON) was also reduced to 70 (figure 2 b-d).

In order to investigate the effect of fluorescent moiety in inducing cyanide as turnover catalyst, the chemodosimeter **CD-2** possessing pyrenylmethyl moiety at N-3 of the naphthimidazolium moiety was studied. The UV-Vis spectrum of solution of **CD-2** exhibited characteristic absorption bands at 335 (ϵ 26,900) and 352 (ϵ 29,500) due to pyrene moiety. The addition of NaCN (10 μM, 1 equiv.) resulted in increase in absorbance at 335 (ϵ 35,800) and 352 (ϵ 39,700) nm with a new band at 400 (ϵ 17,600) nm (figure SI 11b). On excitation of the solution of **CD-2** (10 μM) at 300 nm, the fluorescence spectrum exhibited a structured emission band between 370 – 440 nm, a characteristic of the monomer emission of pyrene moiety and a relatively lower intensity emission band centred at 470 nm. On addition of various anions to the solution of **CD-2**, only cyanide ions showed the enhancement in fluorescence intensity at 470 nm (figure SI 12). On gradual addition of aliquots of cyanide ions to the solution of **CD-2** (10 μM), the fluorescence intensity at 470 nm increased gradually and achieved a plateau after addition of 0.1 equiv. (1 μM) of cyanide ions (figure 3).

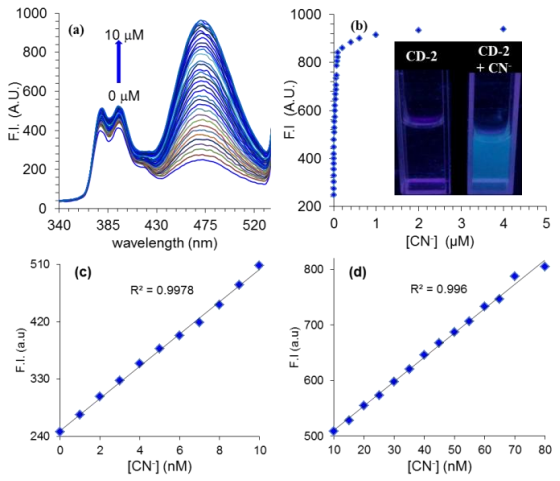

Figure 3. (a) Effect of gradual addition of NaCN on the emission spectrum (λ_{ex} 300 nm) of **CD-2** (10 μM, HEPES buffer - 5% DMSO, pH 7.4); (b) Gradual change in fluorescence intensity of **CD-2** at 470 nm on addition of 0-5 μM NaCN. Inset shows the color of the solution of **CD-2** before and after addition of CN^- (10 μM) under illumination of 365 nm

UV light. (c and d) linear increase in FI with gradual increase in NaCN concentration between 0-10 nM and 10-80 nM, respectively.

This was associated with ~ 10 times increase in fluorescence quantum yield from 0.005 to 0.05 and the resulting solution appeared bluish-green in color under illumination of 365 nm light (inset, figure 3b). The plot of fluorescence intensity vs [CN^-] shows linear relationship between two different concentration ranges i.e. 0-10 nM (R^2 = 0.9978) and 10 nM – 100 nM (R^2 = 0.9960). The minimum limit for the detection of cyanide is 1 nM. TON is found to be ~360 between addition of 0-10 nM cyanide ions and ~70 on further addition of 10-100 nM cyanide ions. These turn over numbers are quite similar to those obtained for chemodosimeter **CD-1**. Therefore, the chemodosimetric behaviour of **CD-1** and **CD-2** remains unaffected by the nature of the signalling moiety.

To explore the selectivity of **CD-1** and **CD-2** towards CN^- ions even in the presence of excess of other anions, the anion interference studies were carried out. For this, cyanide ions (10 nM) were added to the solutions of **CD-1** (5 µM) possessing excess of other anions (100 µM, 10,000 times of cyanide ions) viz. F^-, Cl^-, Br^-, I^-, SO_4^{2-}, AcO^-, ClO_4^-, NO_3^-, HSO_4^-, OH^-, $H_2PO_4^-$ and SCN^- and their emission spectra were recorded. We have found that the concentration of cyanide ions could be determined within 10% error (figure SI 13).

Further, the practical applicability of the **CD-1** and **CD-2** in tap water was tested. The distilled water in water-DMSO (95:5) mixture was replaced by tap water (Table 1). The fluorescence of **CD-1** and **CD-2** was enhanced on addition of specific amounts of cyanide ions. After keeping for ½ h, the fluorescence spectra were recorded for the estimation of cyanide ions. Table 1 reveals that respectively for **CD-1** and **CD-2**, the maximum relative standard deviation is ≤ 1.8% and pooled relative SD (PRSD) is 1.46% and 1.66%. Maximum relative error is ≤ 1.50% and pooled relative error (PRE) is 1.1% and 1.24%. Keeping in view, the lowest permissible limit of cyanide in drinking water being 1 µM, the probes **CD-1** and **CD-2** can be used for determination of cyanide ions in drinking water.

Table 1: Application of **CD-1** and **CD-2** in determination cyanide from tap water

S. No.	NaCN (nM)	CD-1 conc. ± SD[a] (nM) / relative error	CD-2 Conc. ± SD[a] (nM) / relative error
1	2	2.05 ± 0.04 / 1.41	2.06 ± 0.03 / 1.23
2	5	5.16 ± 0.07 / 0.96	5.12 ± 0.08 / 1.25
3	10	10.46 ± 0.2 / 1.22	11.23 ± 0.21 / 1.50
4	20	19.65 ± 0.3 / 1.16	20.7 ± 0.36 / 1.25
5	50	49.72 ± 0.6 / 0.83	49.9 ± 0.77 / 1.14
6	100	101.30 ± 1.4 / 0.99	104.9 ± 1.54 / 1.06

a Average ± standard deviation of three determinations

X-ray crystal structures of CD-1 and its hydrolysis product 4

In order to confirm the structures of one of the probes and the hydrolysed product formed after its ring opening with cyanide ion and to evaluate the intermolecular interactions between the molecules, the X-ray crystal structures of **CD-1** and formamide **4** were determined (figure 4). **CD-1** crystallizes with two molecules of acetonitrile and a PF_6^- anion in the asymmetric unit. The nitrophenyl ring is *gauche* while anthracene ring is perpendicular to the central naphth-imidazole ring (dihedral angles being 49.76(5) and 89.12(4)°, respectively). On the other hand the nitrophenyl ring is almost perpendicular to the anthracene ring (dihedral angle being 73.52(6)°). In formamide **4**, nitrophenyl and anthracene rings become *gauche* to the naphthalene ring (dihedral angles 55.47(1) and 62.15(1)°, respectively while nitrophenyl and anthracene rings become parallel to each other (dihedral angle 6.84(1)°).

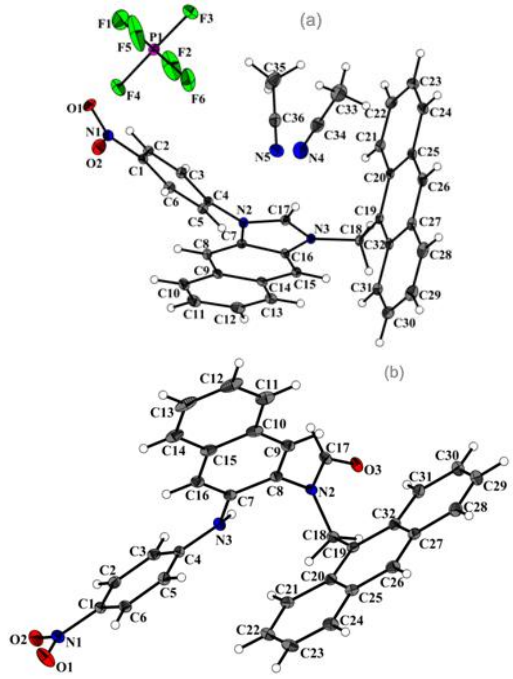

Figure. 4 ORTEP diagrams showing the labeling scheme, of (a) **CD-1**, along with two acetonitrile molecules and PF_6^- anion, (b) formamide **4**

In crystal of **CD-1**, two acetonitrile (ACN) molecules are oriented perpendicular to each other and are having supramolecular interactions with **CD-1**. The most important interactions are, the type IV, lone pair…π interactions[25] between the acetonitrile nitrogen atoms and (hetero)aromatic rings (figure SI 14). For ACN1, N4----centroid of anthracene ring distance, (D1) is of 3.508(2)Å and distances between the nitrogen atom and atoms forming the central ring of anthracene (d1) are all more than 3.25 Å (sum of the van der Waals radii of C and N) with the shortest being 3.448(3) Å. For ACN2 the N5----centroid of naphthimidazolium ring (D2) is 2.926(2) Å while average N5----C distances (d2) is 3.145(2) Å and two N5…N distances (d3) are 3.106(3) and 3.212(3) Å.

While one of the d3 distances is longer than the sum of the vander walls radii of two N atoms (3.10Å), all the D2 distances are less than sum of the van der Walls radii of C and N. From these two kinds of parameters it may be inferred that the lone pair…π interactions are strong for ACN2 while these are weak for ACN1. In fact the D2 of 2.926(2) Å for ACN2 is much shorter than that found in case of type IV lone pair…π contacts in case of six membered heteroaromatic compounds as reported by Reedjk et. al.[25] Our own CSD search for type IV N…imidazole and imidazolium derivatives shows that there are 277 structures containing at least one RC≡N molecule and one imidazole or imidazolium ring. Out of these, 38 (13.7%) exhibit at least one lone pair…π interaction (D < 4Å) and the minimum distance was found as 3.189 Å [26]. That makes this interaction in the present case as the strongest till date.

The crystal structure of **CD-1** shows stacking down the b axis. Two centrosymmetrically related molecules, owing to their conformation are arranged in such a way so as to create a square shaped pseudo cavity between the dimer, which contains four solvent molecules in the cavity and two PF_6^- molecules are lying on the outskirts of this cavity. They are all held by employing C-H…N, C-H…F and C-H…O H-bonding and above mentioned lone pair…π interactions. Such dimers are subsequently held to each other due to π…π interactions (3.626(2)Å) between the anthracene rings, forming supramolecular chains along the b axis (figure SI 15). Similar π…π interactions between anthracene rings from different molecules may be responsible for the excimer emission appeared in the aggregates of CD-1.

The crystal structure of compound **4** shows strong, mutual H-bonding between two centrosymmetric molecules, using the amide oxygens and amine nitrogen atoms (N3-H3A…O3^{i} 2.942(2)Å, 2.06Å, 176°, i= 3-x,1-y,2-z) generating H-bonded dimers. Such dimers are associated with each other through H-bonding interactions between phenylene carbons C2 and C29 and the nitro groups (C2-H2…O2^{ii} 3.502(2)Å, 2.57Å, 166°, ii=-x+2,-y+1,-z+1; C29-H29…O1^{iii} 3.301(3)Å, 2.53Å,139°, iii = x+1,+y,+z+1). The arrangement gives supramolecular linear tapes running diagonally in the ac plane (figure SI 16)

Mechanism of interaction of chemodosimeters CD-1 and CD-2 with cyanide ions

In the fluorescence spectra of **CD-1** and **CD-2,** the presence of structureless emission bands with respective maxima at ~410 and ~470 nm, unambiguously point to the excimer emission of anthracene moieties[27] in case of **CD-1** and pyrene moieties[28] in case of **CD-2**. In order to rationalise the origin of these excimer emission bands, the dynamic light scattering experiments of the solutions of chemodosimeters **CD-1/CD-2** before and after addition of cyanide ions were performed. DLS experiment of solution of **CD-1** (5 μM, H_2O-DMSO, 95:5) showed the formation of aggregates with mean hydrodynamic diameter of 50 ± 10 nm and 250 ± 30 nm (figure 5a). On addition of 1% cyanide ions to this solution, DLS experiment of the resulting solution demonstrated the formation of aggregates with hydrodynamic diameter 520 ± 50 nm (figure 5b). Similarly, DLS experiments of the solutions of **CD-2** demonstrated the formation of aggregates with hydrodynamic diameter 75 ± 5 nm and 300 ± 30 nm and after addition of 1% cyanide aggregates with hydrodynamic diameter 550 ± 50 nm were observed. The formation of these aggregates was further confirmed by SEM and TEM images of drop casted films prepared from these solutions. SEM and TEM images (figure 5c, 5e) showed the aggregates of **CD-1** with size range 50 - 250 nm. Whereas, in the presence of cyanide ions, the solution of **CD-1** demonstrated the formation of aggregates with larger size 50 - 500 nm (figure 5d, 5f). Similarly, SEM and TEM images (figure SI 17c-17f) of the drop casted thin films of the solutions of chemodosimeter **CD-2** demonstrate the formation of aggregates with sizes between 70 – 200 nm and in the presence of cyanide ions the size of the aggregates increased from 60 – 500 nm. Therefore the chemodosimeters **CD-1** and **CD-2** underwent aggregation in HEPES buffer, where the π- π interactions between anthracene/pyrene moieties (also evident from X-ray structure of **CD-1**) from two different molecules resulted in excimer emission band.

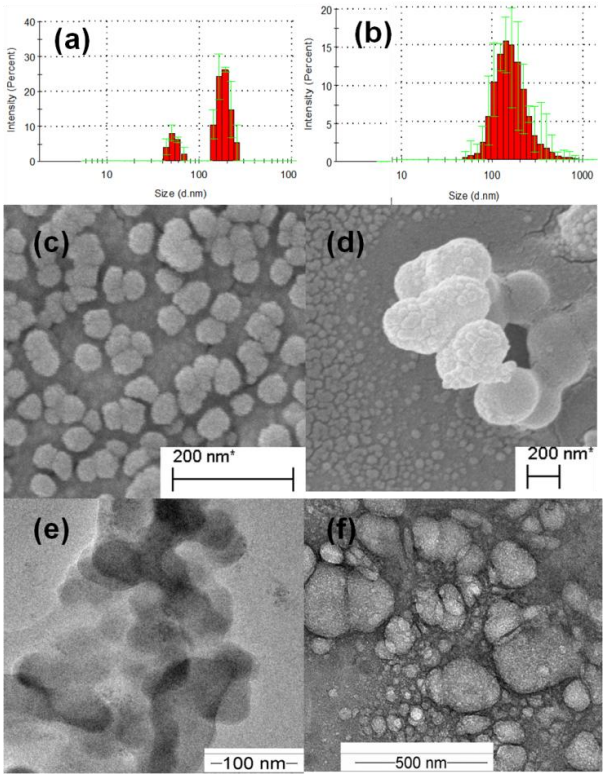

Figure 5 : DLS (a, b), SEM (c, d) and TEM (e, f) studies of **CD-1** (5 μM, H_2O – DMSO 5%) in the absence (a, c, e) and presence (b, d, f) of CN^-

The increased sensitivity and selectivity of such nano-aggregates towards variety of stimulants has been well reported in the literature[29]. Therefore, in case of **CD-1** and **CD-2**, the molecules undergo aggregation to form the weakly fluorescent organic particles, which undergo cyanide ions facile catalytic hydrolysis and the hydrolysed products again aggregated into organic particles.

Based on these experiments and fluorescence studies, the mechanism of interaction of cyanide with **CD-1** and **CD-2** is proposed in scheme 3. On addition of HEPES buffer to the solutions of **CD-1** or **CD-2** in CH_3CN, the molecules undergo aggregation to particles with mean sizes 70-100 nm. On addition of cyanide ions to this solution, the molecules in these aggregates undergo addition of cyanide ion at C-2 of the naphthimidazolium moiety which subsequently undergoes hydrolysis in the presence of water to give heterocyclic ring opened molecules **4** or **5** and cyanide ion becomes free to add on another molecule of naphthimidazolium moiety. The molecules **4** and **5**, again reorganised themselves to form aggregates. On addition of 0.01% to 0.1 % cyanide to chemodosimeter solution, the TON of cyanide is ~360, but on addition of cyanide between 0.1 - 1%, the TON is reduced to ~ 70. The instantaneous formation of molecules **4** / **5** during the catalytic process is also confirmed by the comparison of fluorescence spectra of **CD-1** / **CD-2** obtained after addition of 1 equiv. of cyanide ions with that of molecules **4**/**5**.

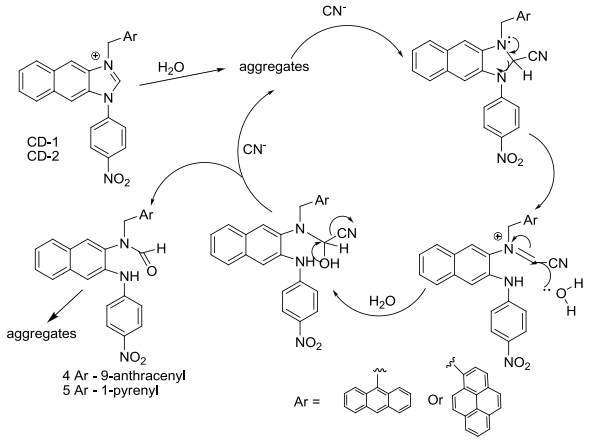

Scheme 3: The proposed mechanism for transformation of chemodosimeters **CD-1** and **CD-2** by cyanide ions

The catalytic mechanism has been further confirmed by the time dependent kinetic study of **CD-1**. On addition of 5 nM cyanide ions to the solution of **CD-1** and recording the spectrum after every 3 minutes demonstarted the gradual increase in FI up to 15 minutes and then plateau was achieved (figure SI 18). The cyanide mediated rate[30] of hydrolysis of chemodosimeter **CD-1** was calculated from time versus fluorescence intensity plot at 420 nm and is found to be K = slope x 2.303 = 12.64 s^{-1}.

In order to have further insight into the mechanism of interaction of cyanide ions with **CD-1** and **CD-2,** the 1:1 solution of **CD-1 +** CN^- and **CD-2** + CN^- (10 μM) were extracted with ethyl acetate and the respective compounds **4** and **5** were isolated**.** The fluorescence spectrum of **4** was found to be comparable with that of the 1:1 solution of **CD-1** and cyanide ions (figure SI 19a). Similarly, the fluorescence spectrum of formamide **5** was found to be comparable with that of the 1:1 solution of **CD-2** and cyanide ions (figure SI 19b). The solutions of **4** and **5** did not undergo any change in fluorescence on addition of excess of cyanide ions.

Analysis of cyanide ions in blood serum

The blood serum has thousands of biomolecules at different concentrations. One of the application of chemodosimeters **CD-1** and **CD-2** can be observed if these can be used for estimation of cyanide concentration in blood serum. For this purpose, the solutions of **CD-1** and **CD-2** containing 10% (v/v) human blood serum were prepared. On addition of blood serum (BS), the fluorescence intensity of **CD-1** at 430 nm is only marginally increased and provides opportunity for estimation of cyanide ions in blood serum. On gradual addition of cyanide ions to the solution of **CD-1** + blood serum, the fluorescence intensity of the resulting solution increases gradually (figure 6) before it achieves a plateau at 1 equiv. of cyanide ions. However, **CD-1** in the presence of blood serum becomes slightly less sensitive to the presence of cyanide ions and the minimum detection limit for the estimation of cyanide ions is raised to 2 nM from that of 1 nM observed in the absence of blood serum.

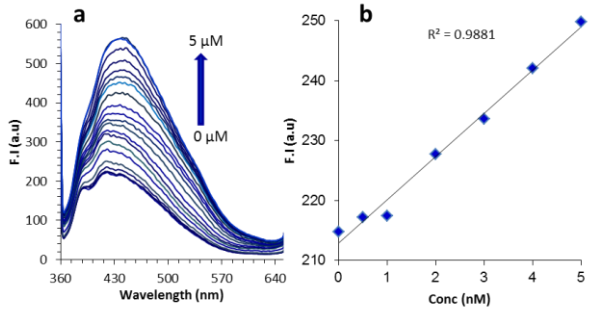

Figure 6. (a) Effect of gradual addition of NaCN aliquots on emission spectrum (λ_{ex} 320 nm) of **CD-1** (5 μM) + blood serum, (b) linear increase in FI with gradual increase in NaCN concentration between 0 - 5 nM respectively.

On addition of cyanide to the solution of **CD-2**, the fluorescence intensity is dramatically increased with emission maxima at 470 nm. However, in the presence of blood serum, the maxima is shifted to 400 nm. Therefore, chemodosimter **CD-2** shows strong interactions with blood serum and cannot find application for the estimation of cyanide ions from the blood serum.

Bioimaging of cyanide ions in live C6 glioma cells

To demonstrate the applications of chemodosimeters **CD-1** and **CD-2** in live cell imaging, the glial cells of the rat brain (C6 glioma cells) were incubated with **CD-1** and **CD-2** in separate experiments.

MTT assay with C6 cells shows no significant difference in the proliferation of the cells in the absence or presence of 5-50 μM of **CD-1** and **CD-2** (figure SI 20). Therefore, **CD-1** and **CD-2** have very low toxicity towards C6 glioma cell lines.

C6 glioma cells themselves and after incubation with **CD-1** and **CD-2** (5 μM) (30 min.), on excitation with 405 nm laser

exhibited no fluorescence (figures SI 21, 22, figures 7a-b). These cells pre-treated with **CD-1** and **CD-2** (5 μM) were loaded with cyanide ions (10 nM and 100 nM) solutions for half an hour. The cells pre-treated with **CD-1** and **CD-2** and then loaded with 10 nM cyanide ions show significantly high fluorescence both in the blue and green windows of the detector (figure SI 21, 22, figure 7c). The increase in concentration of cyanide ions from 10 nM to 100 nM does not cause any further significant increase in the intensity of fluorescence (figure SI 22d). Chemodosimeter **CD-2** is more sensitive to cyanide ions and exhibits significantly large enhancement in fluorescence intensity on treatment with cyanide ions as compared to that observed in case of **CD-1** (figures SI 21, 22). Fluorescent green or blue signals were visible only in the perinuclear region of the cytosol (figure 7c). The permeation of **CD-1** and **CD-2** probably does not take place through the nuclear membrane and as a result nuclear region gave no fluorescence after incubation with **CD-1** and **CD-2** alone or in combination with cyanide (10 nM - 100 nM) ions. Therefore, chemodosimeters **CD-1** and **CD-2** are permeable to C6 cells and can be used for bioimaging of cyanide ions as low as 10 nM concentration. This constitutes first report where 10 nM cyanide ions could be detected in live cell imaging.

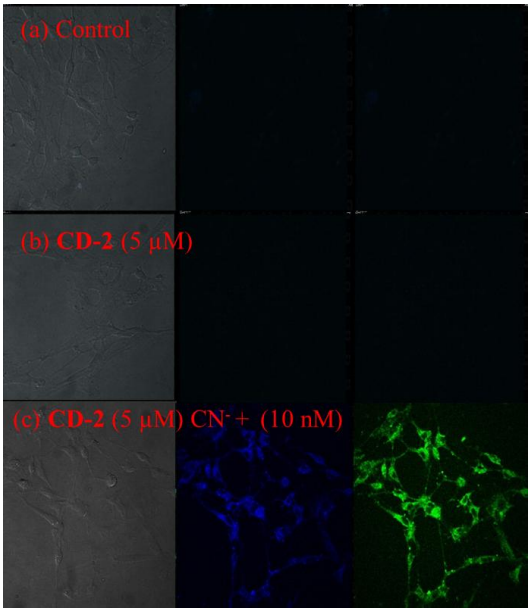

Figure 7. Respective images of C6 glioma cells are as brightfield image and under blue window and green window (a) image of untreated C6 glioma cells, (b) fluorescence image of C6 glioma cells treated with chemodosimeter **CD-2**, (c) fluorescence image of C6 glioma cells treated with **CD-2** and then with CN^- (10 nM).

Experimental

Materials and Reagents

All chemicals were obtained from common suppliers Aldrich, SDFCL, Spectrochem etc. and were used without further purification.

Instrumentation

^1H and ^{13}C NMR spectra were recorded on BRUKER-AVANCE-II FT-NMR AL400 and BRUKER Biospin AVANCE-III FT NMR HD-500 spectrophotometers using $CDCl_3$ or DMSO-d_6 as solvent and tetramethylsilane (TMS) as internal standard. Data are reported as follows: chemical shifts in ppm, coupling constants J in Hz; multiplicity (s = singlet, d = doublet, t = triplet, m = multiplet). High resolution mass spectra were recorded on BRUKER DALTONIK micrOTOF-Q11 spectrometer. UV-Vis studies of compounds were performed on SHIMADZU-2450 spectrophotometer, with a quartz cuvette of path length 1 cm. The cell holder was thermostated at 25.0 ± 0.2 °C. The fluorescence spectra were recorded on BH-CHRONOS and Perkin Elmer LS-55 fluorescence spectrophotometers with a quartz cuvette of path length 1 cm. The cell holder was thermostated at 25.0 ± 0.2 °C. Confocal microscopy imaging was performed on NIKON AIR confocal laser scanning microscope using multiline Argon laser with excitation at 405 nm. Cell imaging was carried out using Plan Apo 60X oil immersion objective lens. The scanning electron microscope (SEM) images were obtained with a field emission scanning electron microscope SEM JEOL JSM-6610LV. The transmission electron microscope (TEM) images were obtained with JEOL JEM-2100 Electron Microscope. DLS experiments were performed on Malvern-Zetasizer.

X-ray structure determination

Crystals of **CD-1** (**CCDC** 1042262 Formula: C32H22N3O2 1+,F6 P1 1-,2(C2 H3 N1) Unit Cell Parameters: a 9.895(3) b 11.505(5) c 14.869(4) P-1) and formamide **4** (**CCDC** 1042263 Formula: C32H23N3O3 Unit Cell Parameters: a 9.816(4) b 11.381(4) c 13.411(6) P-1) were grown by slow evaporation in acetonitrile – isopropanol mixture. X-ray data of both compounds were collected on a Bruker's Apex-II CCD diffractometer using Mo Kα (λ=0.71069). The data were corrected for Lorentz and polarization effects and empirical absorption corrections were applied using SADABS from Bruker. For **CD-1** a total of 27399 reflections were measured out of which 7472 were independent and 5725 were observed [I>2 σ (I)] for theta 27.90°. For compound **4**, a total of 21829 reflections were measured out of which 5099 were independent and 3749 were observed [I>2 σ (I)] for theta 25°. The structures were solved by direct methods using SIR-92 [31a] and refined by full-matrix least squares refinement methods based on F^2, using SHELX-97[31b]. All non-hydrogen atoms were refined anisotropically. All hydrogen atoms were fixed geometrically with their Uiso values 1.2 times of the phenylene and methylene carbons and 1.5 times of the methyl carbons. All calculations were performed using Wingx[31c] package. Compound **4** showed lot of diffused electron density apart from the well resolved molecule which is due to solvent molecules probably due to highly disordered isopropanol molecules which could not be modeled reasonably well. Therefore they were removed using 'SQUEEZE' routine of the PLATON[31d] software. That improved the R factor, wR and the weighting scheme considerably and the refinement could be converged well. The number of electrons recovered from squeeze matches well with those counted for two isopropanol

and one acetonitrile molecules disordered about the inversion centre. The structure shows SAV of 342 Å3 which is equal to the volume of the voids (345 Å3) created on removing this electron density.

Blood Serum

A real blood sample of a medically fit person was used for the experiments. The blood serum was isolated by centrifugation of the fresh blood sample after fasting at 4000 rpm for 30 min at 4 ^{o}C. The stock solution of the blood serum was prepared in 10 ml volumetric flask by diluting 1 ml of serum with HEPES buffer (0.05 M) at pH 7.40.

Live cell imaging

C6 glioma cells were grown in Dulbecco's modified Eagle's medium (DMEM) supplemented with 10% fetal bovine serum (FBS) and 100 IU/ml penicillin, 100 µg/ml gentamycin and 100 µg/ml streptomycin. These cells were maintained in a humidified environment in an incubator at 37 ^{o}C with 5% CO_2. One day before treatment, a total of 2×105 cells were seeded on to 11 mm glass cover slips into each well of a 24-well plate, and these were grown for 24 h (until 60–70% confluence) and treatment with **CD-1** and **CD-2** was carried out in triplicates in FBS and antibiotic free media (98% media supplemented with 2% DMSO). C6 cells were incubated with **CD-1** and **CD-2** (5 µM) at 37 ^{o}C with 5% CO_2 for 30 min followed by three times wash with 1X phosphate buffered saline (PBS) (pH=7.4) and then treated with cyanide ions (10 nM and 100 nM) for another half an hour by incubating the cells at the same conditions. The cells were then washed three times with 1X PBS (supplemented with 2% DMSO), fixed in ice cold 4% paraformaldehyde. Washed again three times with 1X PBS (supplemented with 2% DMSO), and mounted on glass slides. To investigate the cell proliferation and to test their viability **CD-1**, **CD-2**, compounds **4** and **5**, MTT [3-(4,5-dimethylthiazol-2-yl)-2,5-diphenyltetrazolium bromide] assay with C6 cell lines was also carried out. Cell imaging was carried out using Plan Apo 60X oil immersion objective lens.

UV-Vis and Fluorescence Titrations

The concentration of HEPES buffer (pH 7.04) was 0.05 M. Stock solutions of **CD-1** (1 mM) and **CD-2** (2 mM) were prepared in acetonitrile. For experiments with **CD-1** and **CD-2**, we have taken 3 ml of the solution that contains 15 µL **CD-1** solution in acetonitrile,135 µL of DMSO and 2.85 ml of HEPES buffer (0.05 M, pH = 7.4) in cuvette. Typically, aliquots of freshly prepared standard solutions (10^{-1} M to 10^{-3} M) of sodium salts (NaX), where X = CN^- , F^-, Cl^- , Br^- , I^- , ClO_4^- , NO_3^- , SO_4^{2-}, HSO_4^-, SCN^-, AcO^- and $H_2PO_4^-$ in deionized millipore water were used to record UV-VIS and fluorescence spectra.

Detection limit[24]

The detection limit was calculated based on the fluorescence titration. To determine the S/N ratio, the emission intensity of **CD-1** (5 µM) and **CD-2** (10 µM) without cyanide was measured by 5 times and the standard deviation of blank measurements was determined. Under the present conditions, a good linear relationship between the fluorescence intensity and the cyanide concentration could be obtained in the 0 - 5 nM (R^2 = 0.9892) for **CD-1** and 0-10 nM (R^2 = 0.9978) for **CD-2**. The detection limit was then calculated with the equation:

Detection limit = 3σbi/m

Where, σbi is the standard deviation of blank measurements; m is the slope between intensity versus sample concentration. The detection limit was measured to be 1 nM at S/N = 3.

DLS sample preparation

The stock solutions of **CD-1/CD-2** (1 mM, CH_3CN) and water were filtered through 0.02 micron filter membrane to remove interfering impurities. Solutions of **CD-1/CD-2** (5 µM, H_2O - 5% DMSO) and its mixtures with 1% concentrations of CN^- were prepared. 2 ml of each of these solutions was taken in glass cuvette to record the DLS spectrum at 25 ^{o}C.

SEM and TEM sample preparation

The solutions prepared for DLS experiments were used for SEM and TEM. 10 µl of each of the solution was added on the pre-cleaned surface of the separate glass slide and was allowed to dry in the incubator at 25 ^{o}C. SEM images were taken on SEM JEOL JSM-6610LV after sputtering with Ag or Au. For preparation of samples for recording TEM images, 1 µl of the solution was added on copper grid which was allowed to dry in the incubator at 25 ^{o}C.

Synthesis procedure

Synthesis of 1-(4'-Nitrophenyl)naphthimidazole (**1**). 1-Chloro-4-nitrobenzene (2.8 g, 17.85 mmol), CuI (170 mg, 0.9 mmol) and benzotriazole (212.6 mg, 1.8 mmol) were dissolved in DMSO (8 ml). To this stirred mixture naphthimidazole (2 g, 11.9 mmol) and K-OBu^t (1.6 g, 14.28 mmol) were added under N_2 and resulting solution was heated at 130 ^{o}C for 24h. The reaction mixture was cooled to room temperature and aqueous solution of EDTA (1.2 mmol) was added. The compound was extracted with ethyl acetate (3 × 30 ml). The solvent was distilled off, and residue on column chromatography with hexane-ethyl acetate (3:7) mixture as eluent gave pure compound **1**, yellowish-orange solid (2.4 g). Yield 70 %; M. pt. 128 ^{o}C; ^{1}H NMR (DMSO-d_6, 500 MHz): δ 7.46 – 7.51 (m, 2H, ArH), 8.06 – 8.11 (m, 4H, ArH), 8.37 (d, 2H, *J* = 17.6 Hz, ArH), 8.49 (d, 2H, *J* = 9.0 Hz, ArH), 8.97 (s, 1H, ArH); ^{13}C NMR (DMSO-d_6, 125 MHz): δ 107.7, 117.7, 123.9, 124.7, 125.4, 126.1, 128.3, 128.7, 130.5, 131.1, 132.9, 142.1, 144.4, 145.9, 147.5. HRMS m/z(TOF MS ES$^+$), calculated for $C_{17}H_{11}N_3O_2$, m/z 289.0851; found 290.1102 (100%, M + H^+)

Chemodosimeter CD-1. The solution of **1** (100 mg, 0.35 mmol) and **2** (94 mg, 0.35 mmol) in acetonitrile was refluxed for 24 h under N_2. On completion of the reaction, the reaction mixture was cooled to room temperature and the yellow solid separated was filtered off. The solid was dissolved in methanol (20 ml) and NH_4PF_6 (57 mg, 0.35 mmol) was added and the solution was allowed to stir for 24 h. The solid separated was filtered and was crystallized from acetonitrile to get pure **CD-1**, yellow solid (196 mg); Yield 90%; M.pt. 175 ^{o}C; ^{1}H NMR (CD_3CN, 400 MHz) : δ 6.74 (s, 2H, CH_2), 7.60 - 7.68 (m, 5H, ArH), 7.74 - 7.83 (m, 4H, ArH), 8.20 (d, 1H, *J* = 8.0 Hz, ArH), 8.24 (d, 2H, *J* = 8.4 Hz, ArH), 8.33 (d, 2H, *J* = 7.6 Hz, ArH), 8.37 (d, 2H, *J* = 6.8 Hz, ArH), 8.40 (s, 1H, ArH), 8.59 (s, 1H, ArH), 8.88 (s, 1H, ArH), 8.97 (s, 1H, ArH); ^{13}C NMR (CD_3CN, 100 MHz): δ 44.5, 111.5, 112.3, 120.2, 123.3, 125.5, 125.9, 126.8, 127.7, 128.2,

128.5, 128.6, 129.7, 130.9, 131.4, 131.6, 131.8, 131.9, 132.4, 137.8, 143.8, 148.7; HRMS m/z (TOF MS ES$^+$), calculated for $C_{32}H_{22}F_6N_3O_2P$, m/z = 480.1707 [**CD-1** - PF_6]$^+$; found 480.1649 [**CD-1** - PF_6]$^+$ (100%).

Chemodosimeter CD-2. The reaction of 1-(4-nitrophenyl)naphthimidazole 1 (100 mg, 0.35 mmol) and 1-(bromomethyl)pyrene 3 (104 mg, 0.35 mmol) by the procedure as described for **CD-1** gave pure compound **CD-2**, light yellow solid (204 mg). Yield 90%; M.pt. 154 ^oC; ^1H NMR (DMSO-d_6 + $CDCl_3$, 500 MHz) : δ 6.74 (s, 2H, CH_2), 7.67 - 7.71 (m, 2H, ArH), 8.14 – 8.20 (m, 2H, ArH), 8.23 – 8.29 (m, 6H, ArH), 8.35 – 8.43 (m, 4H, ArH), 8.61 – 8.68 (m, 4H, ArH), 8.78 (s, 1H, ArH), 10.48 (s, 1H, ArH); ^{13}C NMR (DMSO-d_6 + $CDCl_3$, 125 MHz): δ 49.4, 111.8, 112.5, 123.1, 124.2, 124.7, 125.6, 126.0, 126.2, 126.3, 126.5, 127.2, 127.4 127.5, 127.6, 127.7, 127.8, 128.6, 128.8, 129.0, 129.2, 129.3, 130.7, 130.9, 131.2, 131.5, 132.0, 132.1, 138.8, 147.7, 148.5; HRMS m/z (TOF MS ES$^+$): calculated for $C_{34}H_{22}F_6N_3O_2P$, m/z = 504.1707 [**CD-2** - PF_6]$^+$; found 504.1705 [**CD-2** - PF_6]$^+$ (100%).

Compound 4. The solution of **CD-1** (50 mg) and NaCN (1 equiv.) in DMSO-water (1:9) was stirred at room temperature. After 1h, the solid separated was filtered and was crystallized from acetonitrile to get pure **4** (39 mg); 97%; M.Pt. 140 ^oC; ^1H NMR (DMSO-d_6 + $CDCl_3$, 500 MHz): δ 5.93 (s, 2H, CH_2), 6.54 (d, 2H, *J* = 9.0 Hz, ArH), 7.29 – 7.39 (m, 3H, ArH), 7.51 (d, 1H, *J* = 8.0 Hz, ArH), 7.65 – 7.70 (m, 2H, ArH), 7.85 – 7.92 (m, 4H, ArH), 8.25 (d, 2H, *J* = 9.0 Hz, ArH), 8.29 (s, 3H), 8.32 (s, 1H), 8.80 (s, 1H, NH); ^{13}C NMR (DMSO-d_6 + $CDCl_3$, 125 MHz) 39.6, 114.1, 124.4, 125.4, 126.1, 126.6, 127.2, 127.3, 127.6, 127.8, 128.5, 129.3, 130.1, 130.8, 131.0, 131.1, 132.4, 133,2, 136.2, 138.7, 151.0, 163.6; HRMS m/z (TOF MS ES$^+$): calculated for $C_{32}H_{23}N_3O_3Na$,(M + Na^+) = 520.1637; found 520.1622 (25%).

Compound 5. The solution of **CD-2** (50 mg) and NaCN (1 equiv.) in DMSO-water (1:9) was stirred at room temperature. Within an hr, the solid was separated. It was filtered and was crystallized from acetonitrile to get pure compound **5** (39 mg); 97%; M.Pt. 132 ^oC; ^1H NMR (DMSO-d_6 + $CDCl_3$, 500 MHz): δ 5.62 (s, 2H, CH_2), 6.22 (d, 2H, *J* = 9.0 Hz), 6.74 (s, 2H, CH_2), 7.38 (d, 2H, *J* = 7.0 Hz, ArH), 7.40 – 7.45 (m, 2H, ArH), 7.65 – 7.69 (m, 4H, ArH), 7.75 (t, 2H, J = 7.5 Hz, ArH), 7.90 – 8.0 (m, 5H, ArH), 8.10 – 8.20 (m, 7H, ArH), 8.25 (d, 4H, *J* = 9.0 Hz, ArH), 8.28 – 8.43 (m, 6H, ArH), 8.61 (d, 2H, *J* = 9.0 Hz, ArH), 8.64 (s, 1H), 8.67 (d, 2H, *J* = 9.5 Hz, ArH), 8.75 (d, 2H, J = 9.5 Hz, ArH); ^{13}C NMR (DMSO-d_6 + $CDCl_3$, 125 MHz): 46.2, 49.4, 111.8, 112.5, 112.9, 122.7, 123.1, 123.3, 124.1, 124.2, 124.4, 124.6, 124.7, 125.2, 125.5, 125.6, 126.0, 126.2, 126.4, 126.5, 127.2, 127.3, 127.4, 127.5, 127.6, 127.8, 127.9, 128.1, 128.4, 128.6, 128.8, 128.9, 129.0, 129.1, 129.3, 129.6, 130.0, 130.3, 130.5, 130.7, 130.8, 130.9, 131.0, 131.2, 131.5, 131.9, 132.1, 133.2, 133.7, 135.6, 137.8, 138.8, 147.7, 148.5, 151.0, 163.5, 164.4.; Due to existence of mixture of cis and trans isomers, the ^1H and ^{13}C NMR signals are doubled. HRMS m/z (TOF MS ES$^+$): calculated for $C_{34}H_{23}N_3O_3Na$, (M + Na^+) = 544.1637; found 544.1626 (100%).

Conclusions

In conclusion, this manuscript accomplishes first report where recognition of cyanide ions has been achieved through catalytic hydrolysis of the fluorescent chemodosimeters. The aggregates obtained from naphthimidazolium based chemodosimeters **CD-1** and **CD-2** undergo highly selective fluorescence enhancement in the presence of 1-100 nM cyanide ions (0.01% to 1% of probe concentration) with TON between 70-360 and limit of detection 1 nM. **CD-1** can also be used for the determination of cyanide in drinking water and in the presence of blood serum. **CD-1** and **CD-2** also find applications in bioimaging of as low as 10 nM cyanide ions in rat brain C6 glioma cells.

Acknowledgements

We thank DST, India (SR/S1/OC-75/2012) for research grants; UGC for UPE programme to the university and CAS status to the department. RK and SS acknowledge UGC and CSIR for fellowships. Live cell experiments were supported by grant from DBT, India (BT/IN/German/13/VK/2010) to VV.

Notes and references

1 M.Y. Chae, A.W. Czarnik, *J. Am. Chem. Soc*., 1992, 114, 9704.

2 (a) K. K. W. Mak, H. Yanase, R. Renneberg, *Biosensors and Bioelectronics*, 2005, 20, 2581-93; (b) R. M. Manez, F. Sancenon, *Coord. Chem. Rev.*, 2006, **250**, 3081; (c) J. Ma, P. K. Dasgupta, *Anal. Chim. Acta*., 2010, 673, 117; (d) D. T. Quang, J. S. Kim, *Chem. Rev*., 2010, **110,** 6280; (e) X. Chen, T. Pradhan, F. Wang, J. S. Kim, J. Yoon, *Chem. Rev*., 2012, **112**, 1910.

3 (a) J. Du, M. Hu, J. Fan, X. Peng, *Chem. Soc. Rev*., 2012, **41,** 4511; (b) K. Kaur, R. Saini, A. Kumar, V. Luxami, N. Kaur, P. Singh, S. Kumar, *Coord. Chem. Rev*., 2012, **256**, 1992; (c) L. M. Hyman and K. J. Franz, *Coord. Chem. Rev*., 2012, **256,** 2333; (d) H. S. Jung, X. Chen, J. S. Kim, J. Yoon, *Chem. Soc. Rev*., 2013, **42**, 6019; (e) Y. Yang, Q. Zhao, W. Feng, F. Li, *Chem. Rev*., 2013, **113**, 192; (f) F. Wang, L. Wang, X. Chen, J. Yoon, *Chem. Soc. Rev*., 2014, **43**, 4312.

4 (a) A. L. Garner, K. Koide, *Chem. Commun*., 2009, 86; (b) A. L. Garner, K. Koide, *Chem. Commun*., 2009, 83; (c) M. Santra, S. K. Ko, I. Shin, K. H. Ahn, *Chem. Commun.*, 2010, **46**, 3964; (d) F. Song, A. L. Garner; K. Koide, *J. Am. Chem. Soc.*, 2007, **129**, 12354; (e) A. L. Garner, F. Song, K. Koide, *J. Am. Chem. Soc.,* 2009, **131**, 5163; (f) M. E. Jun, K. H. Ahn, *Org. Lett*., 2010, **12,** 2790; (g) M. Pal, K. Parasuraman, K. R. Yeleswarapu, *Org. Lett*., 2003, **5**, 349.

5 (a) Z. Zhou, N. Li and A. Tong, *Anal. Chim. Acta.,* 2011, **702**, 81; (b) M. H. Kim, H. H. Jang, S. Yi, S. K. Chang, M. S. Han, *Chem. Commun*., 2009, 4838; (c) J. Kovács, A. Mokhir, *Inorg. Chem*., 2008, **47**, 1880; (d) Q. L. Wang, H. Zhang, Y. B. Jiang, *Tetrahedron Lett*., 2009, **50**, 29; (e) M. Santra, D. Ryu, A. Chatterjee, S. K. Ko, I. Shin, K. H. Ahn, *Chem. Commun*., 2009, 2115; (f) D. N. Lee, G. J. Kim, H. J. Kim, *Tetrahedron Lett*, 2009, **50**, 4766; (g) J. H. Do, H. N. Kim, J. Yoon, J. S. Kim, H. J. Kim, *Org. Lett.,* 2010, **12** 932.

6 (a) G. D. Muir, *The Royal Chemical Society: London*, 1977; (b) Toxicology Profile for Cyanide, U.S. Department of Health and Human Services: Washington, D.C., 2006; (c) M. A. Cherian, I. J. Richmond, *Clin. Pathol*., 2000, **53**, 794; (d) M. Laforge, H. Gourlain, D. Fompeydie, F. Buneaux, S. W.

Borron, M. J. Galliot-Guilley, *Toxicol. Clin. Toxico*., 1999, **37**, 337.
7 S. I. Baskin and T. G. Brewer, ed. F. Sidell, E. T. Takafuji, D. R. Frenz, TMM publications, Washington DC, 1997, ch.10, pp. 271.
8 (a) S. I. Baskin, J. B. Kelly, B. I. Maliner, G. A. Rockwood, C. K. Zoltani, ed. Shirley, D. T. TMM publications, Washington DC, 2008, ch. **11**, pp. 331; (b) J. L. Way, *Annu. Rev. Pharmacol. Toxicol*., 1984, **24**, 451; (c) C. E. Cooper, G. C. Brown, *J. Bioenerg. Biomembr*, 2008, **40**, 533.
9 J. D. Johnson, T. L. Meisenheimer, and G. E. Isom, *Toxic. Appl. Pharmacol*., 1986, **84**, 464.
10 (a) R. Koenig, *Science*, 2000, **287**, 1737; (b) Ullmann's Encyclopedia of Industrial Chemistry, 6th ed.; Wiley-VCH, New York, 1999.
11 R. M. Glead, W. J. Foley and I. E. Woodrow, F. Muell, *Plant. Cell Environ*., 1998, **21**, 12.
12 Guidelines for water reuse, U.S. Environmental Protection Agency, Washington, DC., EPA/625/R-04/108-(2004).
13 (a) Y. Asano, M. Dadashipour, M. Yamazaki, N. Doi, H. Komeda, *Protein Eng. Des. Sel*., 2011, **24**, 607; (b) R. J. H. Gregory, *Chem. Rev*., 1999, **99**, 3649.
14 (a) R. Jackson, I. Petrikovics, E. P. C. Laic, J. C. C. Yu, *Anal. Methods*, 2010, **2,** 552; (b) C. V. Vinnakota, N. S. Peetha, M. G. Perrizo, D. G. Ferris, R. P. Oda, G. A. Rockwood, B. A. Logue, *Biomarkers*, 2012, **17**, 625.
15 (a) J. Ma, S. I. Ohira, S. K. Mishra, M. Puanngam, P. K. Dasgupta, S. B. Mahon, M. Brenner, W. Blackledge, G. R. Boss, *Anal. Chem*., 2011, **83,** 4319; (b) J. Ma, P. K. Dasgupta, W. Blackledge, G. R. Boss, *Anal. Chem*., 2010, **82**, 6244; (c) Y. Tian, P. K. Dasgupta, S. B. Mahon, J. Ma, M. Brenner, J. H. Wang, G. R. Boss, *Anal. Chim. Acta*., 2013, **768**, 129.
16 (a) R. Jackson, R. P. Oda, R. K. Bhandari, S. B. Mahon, M. Brenner, G. A. Rockwood, B. A. Logue, *Anal. Chem*., 2014, **86**, 1845; (b) B. A. Logue, D. M. Hinkens, S. I. Baskin, G. A. Rockwood, *Crit. Rev. Anal. Chem*., 2010, **40**, 122.
17 F. Wöhler, J. Liebig, *Ann Pharm*., 1832, **3**, 249.
18 (a) S. Pramanik, V. Bhalla, M. Kumar, *ACS Appl. Mater. Interfaces*, 2014, **6**, 5930; (b) S. Khatua, D. Samanta, J. W. Bats, M. Schmittel, *Inorg. Chem*., 2012, **51**, 7075; (c) X. Li, L. Peng, J. Cui, W. Li, C. Lin, D. Xu, T. Tian, G. Zhang, D. Zhang and G. Li, *Small,* 2012, **8**, 612; (d) Y.-K. Tsui, S. Devaraj, Y. P. Yen, *Sensors and Actuator B: Chem*., 2012, **161**, 510; (e) Y. Ding, T. Li, W. Zhu and Y. Xie, *Org. Biomol. Chem*., 2012, **10** 4201; (f) S. Madhu, S. K. Basu, S. Jadhav, M. Ravikanth, Analyst, 2013, **138**, 299.
19 (a) P. Kaur, D. Sareen, K. Singh, *Dalton Trans*., 2012, **41**, 9607; (b) M. Dong, Y. Peng, Y. M. Dong, N. Tang and Y.W. Wang, *Org. Lett*., 2012, **14**, 130; (c) Y. D. Lin, Y. S. Peng, W. Su, C. H. Tu, C. H. Sun; T. J. Chow, *Tetrahedron*, 2012, **68**, 2523; (d) S. J. Hong and C. H. Lee, *Tetrahedron. Lett*., 2012, **53**, 3119; (e) S. H. Mashraqui, R. Betkar, M. Chandiramani, C. Estarellas, A. Frontera, *New J. Chem*., 2011, **35**, 57; (f) Z. Yang, Z. Liu, Y. Chen, X. Wang, W. He, Y. Lu, *Org. Biomol. Chem*., 2012, **10**, 5073.
20 (a) J.L. Sessler, D.G. Cho, *Org. Lett*., 2008, **10**, 73; (b) D.G. Cho, J.H. Kim, J.L. Sessler, *J. Am. Chem. Soc*., 2008, **130**, 12163.
21 (a) Y. Liu, K. Ai, X. Cheng, L. Huo, L. Lu, *Adv. Funct. Mater*., 2010, **20,** 951; (b) X. B. Wang, Y. L. Wang, J. Yang, X. P. Xing, J. Li, L. S. Wang, *J. Am. Chem. Soc*., 2009, **131**, 16368.
22 (a) S. Kumar, P. Singh, G. Hundal, M. S. Hundal, S. Kumar, *Chem. Commun*., 2013, **49**, 2667; (b) S. Kumar, S. Kumar, *Tetrahedron Lett*., 2009, **50**, 4463.
23 (a) W. H. Melhuish, *J. Phys. Chem*., 1961, **65**, 229; (b) J. N. Demas, G. A. Crosby, *J. Phys. Chem*., 1971, **75**, 991.
24 J. Mokac, A. M. Bond, S. Mitchell, G. Scollary, *Pure Appl. Chem*., 1997, **69**, 297.
25 (a) T. J. Mooibroek, P. Gamez, J. Reedijk, *Cryst. Eng. Comm*., 2008, **10**, 1501; (b) M. Egli, S. Sarkhel, *Acc. Chem. Res*., 2007, **40**, 197.
26 A. Kobel-Pollak, C.J. Mathews, S. Verdan, B. Bocquet, X. Melich, A.F. Williams, F. Lavergnat, P.Y. Morgantini, G. Bernardinelli, *New J. Chem*., 2006, **30**, 851.
27 P. P. Neelakandan and D. Ramaiah, *Angew. Chem. Int. Ed*., 2008, **47,** 8407.
28 Z. Zhao, S. Chen, J.W.Y. Lam, Z.Wang, P. Lu, F. Mahtab, H.H.Y. Sung, I.D. Williams, Y. Ma, H.S. Kwok, B.Z. Tang, *J. Mater. Chem*., 2011, **21**, 7210.
29 (a) J. Suk, Z. Wu, L. Wang and A. J. Bard, *J. Am. Chem. Soc*., 2011, **133**, 14675; (b) Q. Zhao, K. Li, S. Chen, A. Qin, D. Ding, S. Zhang, Y. Liu, B. Liu, J. Z. Sun and B. Z. Tang, *J. Mater. Chem*., 2012, **22**, 15128; (c) J. Wang, X. Xu, L. Shi, and L. Li, *ACS Appl. Mater. Interfaces*., 2013, **5,** 3392; (d) A. Singh, T. Raj, T. Aree and N. Singh, *Inorg. Chem*., 2013, **52**, 13830; (e) K. Tayade, A. Kaurb, S. Tetgurea, G. K. Chaitanya, N. Singh and A. Kuwar, *Analytica Chimica Acta*., 2014, **852**, 196.
30 S. Goswami, S. Das, K. Aich, D. Sarkar, T. K. Mondal, *Tetrahedron Lett*., 2014, **55**, 2695.
31 (a) A. Altomare, G. Cascarano, C. Giacovazzo, A. Guagliardi, J. Appl. Crystallogr., 1993, **26**, 343-350; (b) G. M. Sheldrick, Acta Crystallogr. A, 2008, **A64**, 112; (c) L. J. Farrugia, J. Appl. Crystallogr., 1999, **32**, 837; (d) A. L. Spek, Acta Crystallogr A, 1990, **46**, C34.